Mamm Genome (2016) 27:451–459
DOI 10.1007/s00335-016-9653-8

A novel spontaneous mutation of BCAR3 results in extrusion cataracts in CF#1 mouse strain

Tomohiro Kondo[1] · Taketo Nakamori[1] · Hiroaki Nagai[1] · Ai Takeshita[1] · Ken-Takeshi Kusakabe[2] · Toshiya Okada[1]

Received: 23 February 2016 / Accepted: 13 June 2016 / Published online: 30 June 2016

Abstract A substrain of mice originating from the CF#1 strain (an outbred colony) reared at Osaka Prefecture University (CF#1/lr mice) develops cataracts beginning at 4 weeks of age. Affected mice were fully viable and fertile and developed cataracts by 14 weeks of age. Histologically, CF#1/lr mice showed vacuolation of the lens cortex, swollen lens fibers, lens rupture and nuclear extrusion. To elucidate the mode of inheritance, we analyzed heterozygous mutant hybrids generated from CF#1/lr mice and wild-type BALB/c mice. None of the heterozygous mutants were affected, and the ratio of affected to unaffected mice was 1:3 among the offspring of the heterozygous mutants. For the initial genome-wide screening and further mapping, we used affected progeny of CF#1/lr × (CF#1/lr × BALB/c) mice. We concluded that the cataracts in CF#1/lr mice are inherited through an autosomal recessive mutation and that the mutant gene is located on mouse chromosome 3 between D3Mit79 and D3Mit216. In this region, we identified 8 genes associated with ocular disease. All 8 genes were sequenced and a novel point mutation (1 bp insertion of cytosine) in exon 7 of the *Bcar3* gene was identified. This mutation produced a premature stop codon and a truncated protein. In conclusion, we have identified the first spontaneous mutation in the *Bcar3* gene associated with lens extrusion cataracts. This novel cataract model may provide further knowledge of the molecular biology of cataractogenesis and the function of the BCAR3 protein.

✉ Tomohiro Kondo
kondo@vet.osakafu-u.ac.jp

[1] Department of Laboratory Animal Science, Graduate School of Life and Environmental Biosciences, Osaka Prefecture University, 1-58 Rinku Ourai kita, Izumisano, Osaka 598-8531, Japan

[2] Laboratory of Basic Veterinary Science, The United Graduate School of Veterinary Science, Yamaguchi University, Yamaguchi 753-8515, Japan

Introduction

Cataracts are one of the most common eye defects and causes of lens opacity (Liu et al. 2006), which may lead to blindness (Kang et al. 2008). According to the latest assessment, cataracts are responsible for 51 % of blindness worldwide, representing about 20 million people (Quinlan 2015). Causes of cataracts include congenital defects, senility, metabolic disorders and exposure to a variety of physical and chemical agents (Song et al. 1997). Mutations affecting the lens in mice can be identified easily by visual inspection, and a remarkable number of mutant lines have been characterized (Graw 2009). The establishment of an animal model of cataracts is an effective method to elucidate human cataractogenesis (Graw 2004). In particular, mouse models for cataracts are useful for isolating cataract genes and analyzing the mechanism of cataract development (Kondo et al. 2014a), and many types of inherited cataracts exist in mice and have been evaluated developmentally, histologically and genetically (Kohale et al. 2004; Okamura et al. 2003). Cataract lenses display various morphologic features, including the posterior dislocation of the nucleus (Teramoto et al. 2000), swollen lens fibers (Kondo et al. 2011), vacuolation of the epithelium (Maeda et al. 2001) and vacuolation of the lens cortex (Song et al. 1997).

In the present study, we histologically and genetically investigated the characteristics of CF#1/lr mice, a novel mouse cataract model that originated from the CF1 outbred strain.

Materials and methods

Mouse husbandry

This study utilized CF#1/lr mice, which are a new cataract strain derived from the CF#1 strain of mice. In the Central Research Division (Takeda Chemical Industries, Osaka, Japan), mice with cataracts were identified in a colony of CF#1 mice (outbred colony). The cataract mice were isolated from the colony, named CF#1/lr (lens rupture) and bred by inbreeding (more than 100 generations). These animals were obtained in 2003 and are currently bred inhouse at Osaka Prefecture University. Normal BALB/c mice were purchased from CLEA Japan (Tokyo, Japan) and were used for the mating experiment, genomewide screening and histological studies. MSM/Ms mice were kindly donated by Dr. Moriwaki (National Institute of Genetics, Mishima, Japan), and ddY mice were purchased from Japan SLC, Inc. (Hamamatsu, Japan). MSM/Ms, ddY and CF1/b cac mice, which have been previously described (Kondo et al. 2014b), were used as controls in direct sequencing experiments. All mice were maintained under controlled conditions of room temperature (24 ± 1 °C), humidity (55 ± 5 %) and lighting (lights on 0800–2000). The mice received a commercial diet (CE2; CLEA Japan) and water ad libitum. The present study was performed in accordance with the Guidelines for Animal Experimentation of Osaka Prefecture University, Japan.

Observations and histological studies

The mice were observed with the naked eye under non-anesthetic conditions more than once a week after their eyes opened at approximately 2 weeks old. For the histological studies, 2-, 3-, 4-, 5-, 10- and 14-week-old CF#1/lr mice and 14-week-old BALB/c mice were used. Under isoflurane anesthesia, the mice were infused with heparin–saline followed by 10 % neutral-buffered formalin. The eyes were then removed and immersed in the same fixative for 2 days. The eyes were dehydrated by a graded series of ethanol, soaked in butyl alcohol and embedded in paraffin (Tissue Prep; Fisher Scientific, NJ, USA). Sections (4 μm thick) were cut in a plane perpendicular to the anteroposterior axis of the eye and stained with hematoxylin and eosin.

Mating experiment

To elucidate the mode of inheritance, cataract mice were mated with wild-type BALB/c mice in order to obtain heterozygous mutants. Heterozygous mutants were then mated in order to obtain the segregation ratio of affected and unaffected mice. The incidence of lens opacity was determined with the naked eye by visual examination more than once a week from 2 weeks until 5 months of age.

Linkage analysis

Genomic DNA was extracted from the tail of affected backcrossed progeny [CF#1/lr mouse × (CF#1/lr mouse × BALB/c mouse)]. For linkage analysis of up to 2–4 per chromosome, polymorphic microsatellite markers (Sigma Aldrich Japan, Tokyo, Japan) were selected. These markers had typed polymorphisms between CF#1/lr and BALB/c mice. For the primary check, 21–61 DNA samples from affected mice were used. For the secondary check, 5 microsatellite markers on chromosome 3 (Chr 3) and 250 DNA samples from affected mice were used (Table 1). PCR was performed with a thermocycler (GeneAtlas; Astec, Fukuoka, Japan), and products were analyzed by electrophoresis on a 1.5 % agarose gel. The significance of linkage was evaluated by a Chi-square test of independence (degree of freedom = 1) of frequencies of hetero- and homozygote in the affected backcross mice.

Direct sequencing

Total RNA was extracted from the lens of CF#1/lr, MSM/Ms, ddY and CF1/b cac mice using TRIzol reagent (Life Technologies, NY, USA) according to the manufacturer's protocol. Total RNA was resuspended in diethyl-pyrocarbonate-treated water. Single-strand cDNA was synthesized using a PrimeScript 1st strand cDNA Synthesis Kit (Takara Bio, Otsu, Japan). Primers were designed from known sequences (http://www.ncbi.nlm.nih.gov/) to amply contain the coding regions of the mouse *Bcar3* (Table 2). PCR was performed using PrimeSTAR GXL DNA Polymerase (Takara Bio). PCR products were purified using a NucleoSpin Gel and PCR Clean-up (Macherey–Nagel; Duren, Germany) and prepared for DNA sequencing on an ABI 3130 Genetic Analyzer (Applied Biosystems, CA, USA) using a BigDye Terminator v 3.1 Cycle Sequencing Kit (Applied Biosystems). To confirm mutations in the genomic DNA, primers were designed to span exon7 of the *Bcar3* gene and internal primers were used for sequencing (Table 2).

Results

Macroscopic observation

CF#1/lr mice are shown in Fig. 1. Characteristics of this cataract mouse were opacity of the lens (Fig. 1a) and white fragments in the posterior region of the eye (Fig. 1b). Until

Table 1 Linkage analysis of cataract gene on chromosome 3 of affected backcross progenies

Marker	Position (cM)	No. affected		χ^2
		CF1/CF1 allele	CF1/BALB allele	
D3Mit158	48.13	239	11	207.936
D3Mit79	52.00	245	5	230.400
D3Mit216	54.48	249	1	246.016
D3Mit348	56.07	248	2	242.064
D3Mit254	61.32	237	13	200.704

Table 2 Sequencing primers of *BCAR3*

	Primer sequence 5′–3′	Product size
1F	CTGAACCGGCAATCCCGGAC	461
1R	AGCAGCTCCTCCTCCAATTC	
2F	AAGGAGAGGCACATCATGGAC	588
2R	GCCACTCTTCTCTTTATTCCTGA	
3F	AGACGTGGTGAAGAGGCTGA	552
3R	GATGGCCCATTCTGTTTGGC	
4F	AAGCTTCCCATGCAAGCCCA	555
4R	CTTATTGAGGGTACCCGCTCG	
5F	CTGGACATCATCGAGAGGCA	459
5R	CCTGGCTGTTGCCAAGTGAT	
6F	AATGTGTCAGTCCCTCTGCTG	468
6R	TGTTAGCGGCTTGTATCCTGT	
Genome-F	GGACGCCTTCACAGTGTTCT	961
Genome-R	ATCCCACACCTGCGTTACTG	
Internal-R	TGAGCCAGGGAGATGGAGAG	(422)

3 weeks of age, CF#1/lr mice did not show opacity of the lens. Opacity appeared in mice at 4 weeks of age, and the rate of opacity was 22.2 %; this gradually increased to more than 50 % at 6 weeks of age (50.9 %). All mice were completely affected by 14 weeks of age. There were no significant differences in incidence and the age of onset between male and female mice.

Histological findings

The lens of 2-week-old CF#1/lr mice showed no obvious pathologic changes (Fig. 2a, b). In the equator region of the lens of 3-week-old mice, lens fibers were vacuolated (Fig. 2c, d). At 4 weeks of age, vacuole denaturation increased in size and some of the lens fibers were swollen (Fig. 2e, f). At 5 weeks of age, the lens ruptured at the posterior pole and the nucleus was dislocated (Fig. 2g, h). In 14-week-old CF#1/lr mice, the lens nucleus was completely extruded (Fig. 2i), while in BALB/c mice, the lens was normal (Fig. 2j). Morphologic abnormalities were not observed in areas besides the lens, such as the retina or the cornea (Fig. 3).

Linkage analysis

Heterozygous progeny from CF#1/lr and wild-type BALB/c mice was phenotypically normal. The ratio of affected to unaffected mice in the offspring of heterozygous mutants was approximately 1:3 [36 (female, 16; male, 20):107 (female, 46; male, 61)]. This result indicates that the mode of inheritance was autosomal recessive and the causative

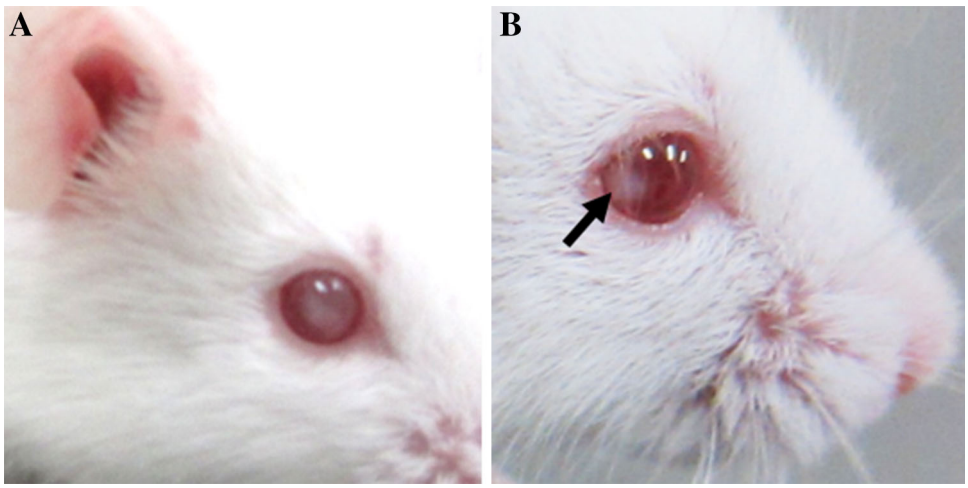

Fig. 1 Macroscopic features of CF#1/lr mice. **a** Extensive opacity is observed in the eye. **b** White fragments (*arrow*) are observed in the posterior region of the eye

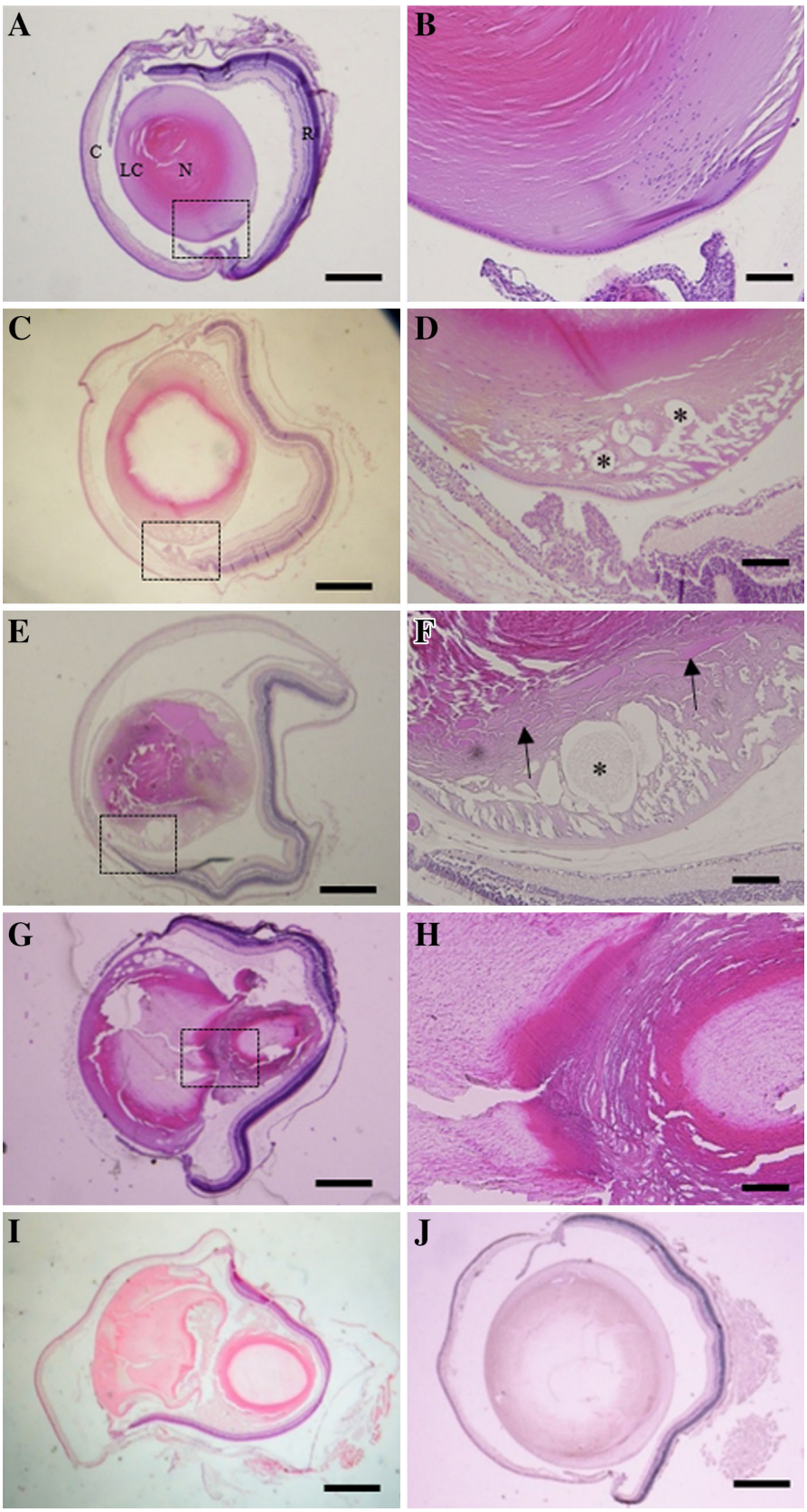

Fig. 2 Lens of CF#1/lr mice (**a** through **i**) and BALB/c mice (**h**). **a**, **b** Lens of a 2-week-old CF#1/lr mouse is normal in appearance. **c**, **d** Equator region of the lens of a 3-week-old CF#1/lr mouse demonstrates vacuoles (*asterisks*) in the lens cortex. **e**, **f** A 4-week-old CF#1/lr mouse exhibits bigger vacuole denaturation (*asterisks*) in the lens cortex. In addition, swelling (*arrows*) and abnormal arrangement of the lens fibers are present. **g**, **h** Posterior region of the lens of a 5-week-old CF#1/lr mouse. The posterior pole is ruptured and the lens nucleus is dislocated. **i** A 14-week-old CF#1/lr mouse shows complete extrusion of the lens nucleus. **j** The eye of a 14-week-old BALB/c mouse is normal. *C* cornea, *LC* lens cortex, *N* lens nucleus, *R* retina. *Scale bars* 500 μm (**a**, **c**, **e**, **g**, **i**, **j**) or 100 μm (**b**, **d**, **f**, **h**)

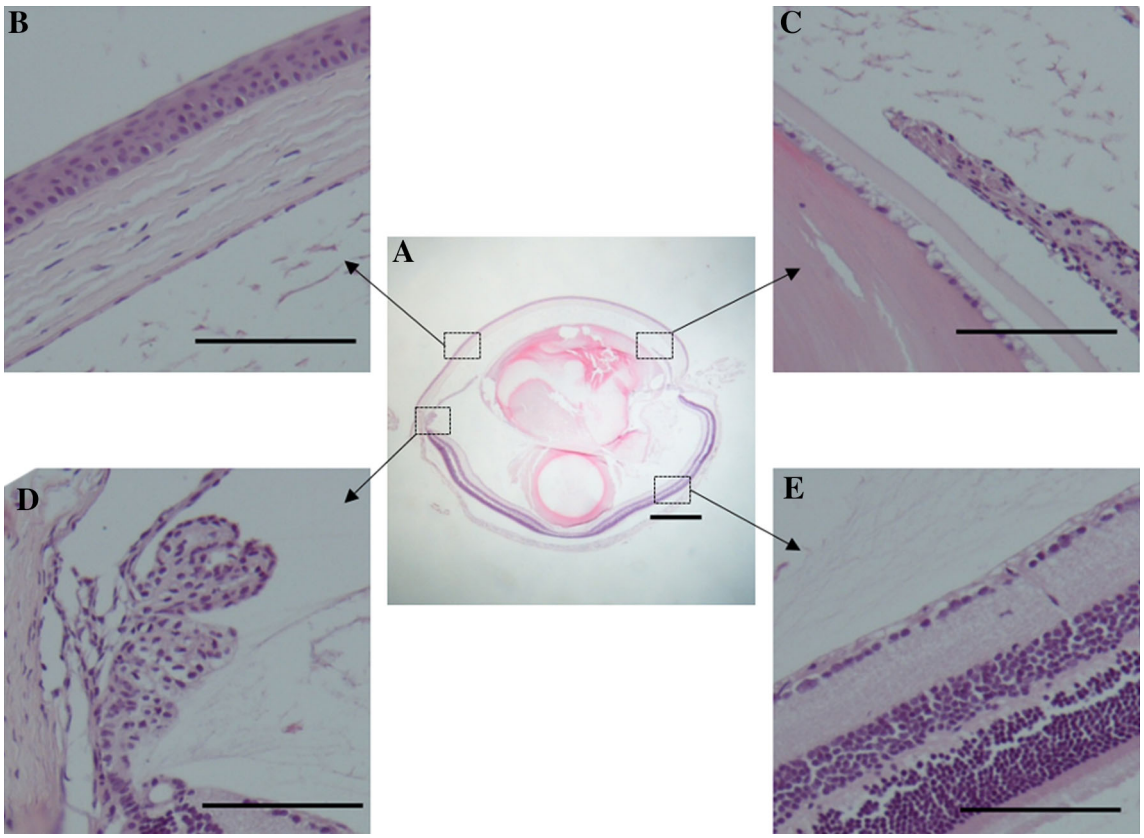

Fig. 3 Eyes of 10-week-old CF#1/lr mice. **a** Whole eye, **b** cornea, **c** iris, **d** ciliary body, **e** retina. Morphologic abnormalities were not observed in areas besides the lens. *Scale bars*, 500 μm (**a**) or 100 μm (**b–e**)

mutation was single. As such, affected backcrossed progeny [CF#1/lr × (CF#1/lr × BALB/c)] was used for linkage analysis. As the result of a genome-wide linkage analysis, the mutation was mapped to chromosome 3, close to the marker D3Mit348. This indicates that there is a linkage between the mutant gene and Chr 3. Therefore, further linkage analyses were carried out with 5 microsatellite markers (D3Mit158, D3Mit79, D3Mit216, D3Mit254 and D3Mit348). The results of further mapping are given in Table 1. The χ^2 values for these five polymorphic microsatellite loci ranged from 200.70 to 246.01. All 24 offspring arose as a result of a single crossover event (Fig. 4a). Analysis of the haplotype distribution pattern allowed for the mutated gene to be localized at the 2.4 cM region between D3Mit79 and D3Mit216. The physical distance between D3Mit79 and D3Mit216 was 4.8 Mb (Fig. 4b).

Direct sequencing

Sequencing of the *Bcar3* cDNA identified a 1-bp insertion of cytosine in exon 7 at position 1452 (Fig. 5a). In addition, further mutations, such as single nucleotide deletion, were not detected after the insertion. This insertion results in a frameshift mutation, leading to a premature stop codon and a truncated protein (Fig. 5b). This mutation was not detected in other strains (CF1/b cac, MSM/Ms and ddY). The same mutation was confirmed in the genomic DNA.

Discussion

The present study revealed that a new cataract model, the CF#1/lr mouse, is characterized by lens rupture at the posterior pole at 4–14 weeks after birth. The mutation is inherited in an autosomal recessive fashion, and the anomaly carried a single nucleotide insertion in the *Bcar3* gene, leading to a premature stop codon and a truncated protein.

The 4 major morphologies of mouse cataracts are nuclear, cortical, capsular–epithelial and lens extrusion (Smith et al. 1997). The various abnormal changes in cataract lenses include nuclear remnants in the lens fibers (Graw et al. 2002), vacuolated epithelial cells (Kondo et al. 2010; Singh et al. 1995), degeneration of cortical fibers, progressive condensation of the nucleus (Narita et al. 2002) and degeneration of the lens capsule. A lens extrusion cataract involves the thinning and rupture of the posterior lens capsule, leading to the extrusion of lens cortical

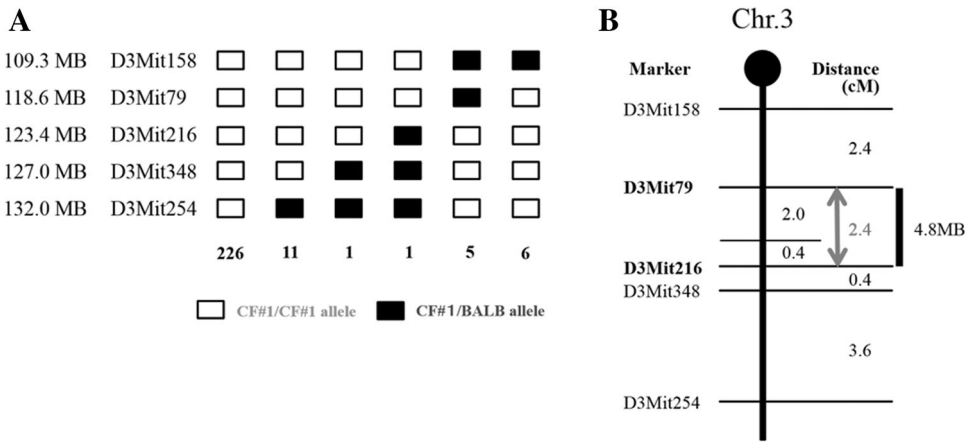

Fig. 4 **a** Distribution of haplotypes in a set of 250 affected offspring from genetic backcrossing (CF#1/lr × [CF#1/lr × BALB/c]). The typed loci are listed on the left. *Columns* denote specific chromosomes identified in affected backcrossed progeny. Values at the bottom of the figure are the number of progeny that inherited the indicated chromosomal haplotype from the F1 parent. *Black squares* represent the CF#1/BALB allele; *white squares* represent the CF#1/CF#1 allele. **b** Genetic linkage map of chromosome 3. Typed loci are listed on the left of the chromosome, and values to the right are distances between loci. The map shows the location of the cataract gene of CF#1/lr mice (*arrow*)

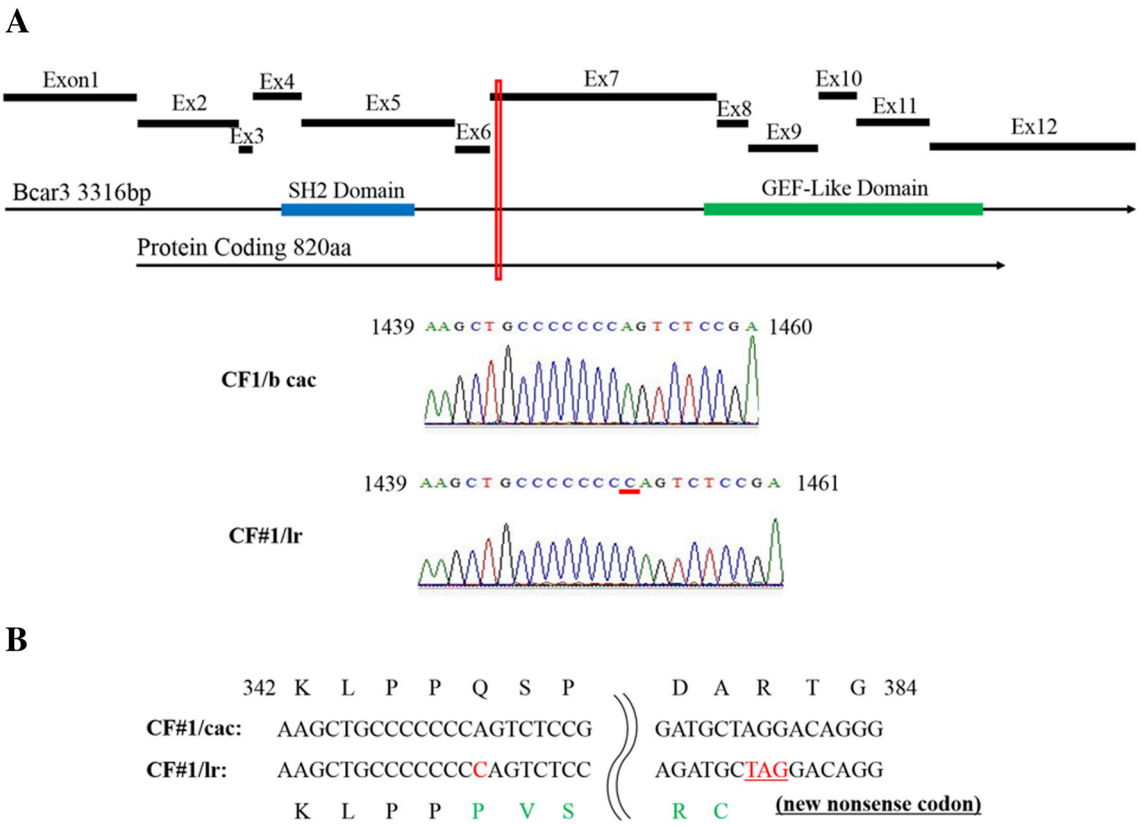

Fig. 5 CF#1/lr mutation affects the Bcar3 gene. **a** Exon structure of Bcar3 cDNA is shown. Sequence analysis demonstrates a cytosine insertion at cDNA position 1452, leading to a subsequent amino acid exchange. **b** Amino acid exchanges from 346 to 381, and codon 382 becomes a premature stop codon

material into the vitreous (Smith et al. 1997). In CF#1/lr mice, the lens fiber cells formed around the equator were vacuolated and swollen. The posterior lens capsule was ruptured and the lens nucleus was extruded. These results suggest that the abnormal lens feature of CF#1/lr mice is a lens extrusion cataract.

In the 4 major morphologies of mouse cataracts, reports of lens extrusion cataracts constitute the fewest (Smith et al. 1997). In humans, it is reported that lens rupture occurs in addition to renal failure in Alport syndrome (Agrawal et al. 2015). Moreover, external injuries have been reported as causes of lens rupture (Gray et al. 2011). Also in mice, several reports regarding lens extrusion cataracts are available. Abi2 knockout mice were found to display rupture of the posterior lens capsule at the time of birth. This anomaly occurred due to abnormal lens fiber arrangement during development and failure of lens suture formation (Grove et al. 2004). An RLC mouse was also reported to exhibit lens rupture. This mouse showed rupture of the posterior capsule around 50 days after birth and showed abnormal arrangement of the lens fibers at the newborn stage (Teramoto et al. 2000). We did not observe abnormal morphologic changes in the 2 weeks after birth, suggesting that CF#1/lr mice have normal lens fiber arrangement during development.

In this study, we found that the causative gene of cataract in CF#1/lr mice lies on chromosome 3, between D3Mit79 and D3Mit216 (Fig. 4). In this region, we picked 8 genes (*Cnn3*, *Abcd3*, *Arhgap29*, *Abca4*, *Dnttip2*, *Bcar3*, *Fnbp1 l*, *Pde5a*) associated with ocular disease (Table 3). Sequence analysis was performed with 8 genes. We discovered a 1-bp insertion of cytosine in exon 7 at position 1452 bp of *Bcar3*. This mutation was not detected in other strains, and the other 7 genes showed no mutations in their protein coding regions; thus, it is assumed that *Bcar3* is the causative gene of CF#1/lr mice. This insertion results in a frameshift mutation and produces a premature stop codon and a truncated protein.

BCAR3 is a 95-kDa protein with an amino-terminal SH2 domain and carboxyl-terminal domain homologous to Ras family guanine nucleotide exchange factors (GEF-like domain) (Gotoh et al. 2000; Vanden Borre et al. 2011). BCAR3 binds to p130Cas (Bcar1), a focal adhesion adapter protein. p130Cas and BCAR3 bind tightly to each other through their c-terminal domains, thus potentially connecting their associated signaling networks (Wallez et al. 2014). This complex signaling regulates epithelial and mesenchymal cell adhesion, motility and responses to growth factors (Makkinje et al. 2012). BCAR3 is expressed strongly in lens epithelial cells found around the equator, known as the transitional zone (McAvoy et al. 1999; Near et al. 2009). In this region, the differentiation of lens epithelial cells into lens fiber cells involves the loss of cell nuclei and cell organelles (Bassnett and Mataic 1997). Since the first abnormality observed was lens fiber vacuolization and swelling in the lens equator, we speculated that alteration in BCAR3 function disrupts normal differentiation of lens epithelial cells to lens fiber cells. Subsequently, abnormal lens fiber cells were less able to interact normally with lens fiber cells, lens epithelial cells and the posterior lens capsule. Finally, the posterior lens capsule was ruptured and the lens nucleus was extruded (Fig. 6).

It is reported that BCAR3 knockout mouse exhibits the pathology of lens extrusion. This mouse presents with vacuolization and liquefaction of the lens cortex at 3 days after birth. Lens rupture with extrusion of cortical fiber material is detected at 24–33 days after birth. Other phenotypic alterations observed in adult BCAR3 knockout mouse included abnormally deep anterior chambers and anterior synechiaes covering the trabecular meshwork, ectropion uveae and mild to moderate retinal ganglion cell loss. Morphologic abnormalities are restricted to the eye (Near et al. 2009).

Similarities and differences exist between this spontaneous mutation mouse and BCAR3 knockout mice. Morphological characteristics of the two strains are very similar. For example, first vacuolization was observed in the lens cortex and successively the lens ruptured at the posterior pole. Also, abnormalities were limited to ocular disease. However, the two strains differ greatly in the age of onset. BCAR3 knockout mice presented with vacuolated lens fiber 3 days after birth, and lens rupture with extrusion

Table 3 List of picked 8 genes located in refined cataract locus between 118.6 and 123.4 Mb on chromosome 3

NCBI Gene ID	Symbol	Location (Mb)	Description
71994	Cnn3	121.42–121.47	Calponin 3, acidic
19299	Abcd3	121.75–121.81	ATP-binding cassette, subfamily D (ALD), member 3
214137	Arhgap29	121.95–122.01	Rho GTPase-activating protein 29
11304	Abca4	122.04–122.18	ATP-binding cassette, subfamily A (ABC1), member 4
99480	Dnttip2	122.27–122.28	Deoxynucleotidyltransferase, terminal, interacting protein 2
29815	Bcar3	122.41–122.53	Breast cancer anti-estrogen resistance 3
214459	Fnbp1 l	122.53–122.61	Formin-binding protein 1-like
242202	Pde5a	122.72–122.85	Phosphodiesterase 5A, cGMP-specific

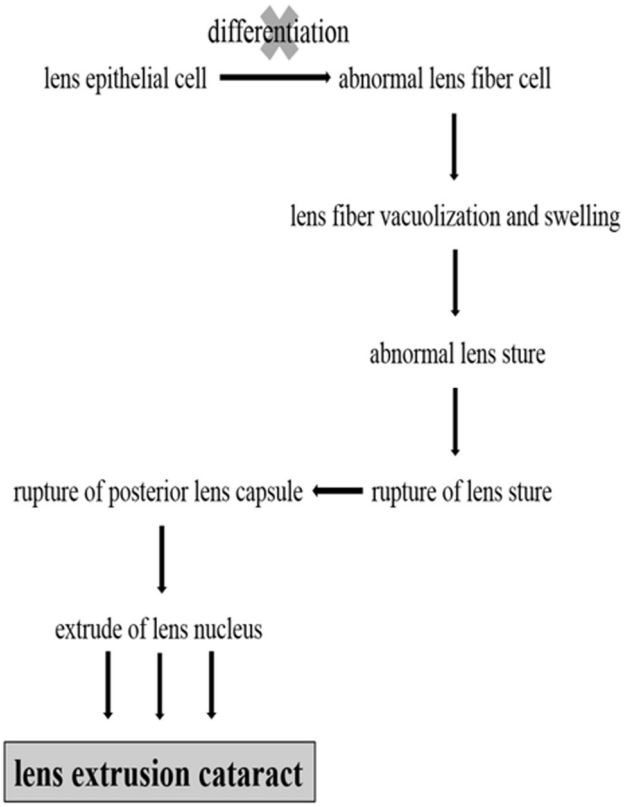

Fig. 6 Possible mechanism of lens extrusion cataract formation

of cortical fiber material was detected at 24–33 days after birth (Near et al. 2009). In contrast, in CF#1/lr mice, the lens fiber was vacuolated at 3 weeks after birth and lens rupture with extrusion of cortical fiber material was detected from 5 weeks after birth. Moreover, visual observation of CF#1/lr mice revealed that all mice developed cataract by 14 weeks of age. In CF#1/lr mice, BCAR3 lacks the GEF-like domain and retains the SH2 domain (Fig. 5a). It is reported that BCAR3 deletion constructs lacking the GEF-like domain have demonstrated a loss of BCAR3-induced cell motility (Cai et al. 2003; Schrecengost et al. 2007). Protein tyrosine phosphatase α (PTPα) regulates integrin signaling, focal adhesion formation and migration. BCAR3 forms a molecular bridge between phospho-PTPα and p130Cas with the SH2 domain of BCAR3 binding to phosphoTyr789 on PTPα and the GEF-like domain of BCAR3 associating with the C-terminal region of p130Cas (Mace et al. 2011; Sun et al. 2012). Interestingly, however, not all BCAR3-associated signaling requires formation of a BCAR3-p130Cas complex. BCAR3-mediated p130Cas phosphorylation requires the amino-terminal BCAR3 SH2 domain, but occurs in the absence of the GEF-like domain, indicating its independence of BCAR3-p130Cas complex formation (Vanden Borre et al. 2011). We have identified that the delay in onset time of CF#1/lr mice might have been caused by disruption of many BCAR3-associated signaling and remaining the few BCAR3-associated signaling. In addition, BCAR3 knockout mice are reported to be on 129 background strains, whereas CF#1/lr mice are on the CF#1 strain; thus, the apparent difference may be due to differences in genetic background. If future studies demonstrate that the function of BCAR3 is not completely knocked out, the usefulness of this model will be considered enhanced.

In conclusion, we report here the first spontaneous mutation in the *Bcar3* gene leading to lens rupture. The CF#1/lr mouse represents an exciting tool for studying the molecular biology of cataractogenesis. Moreover, CF#1/lr mice represent a useful new cataract model and will enable investigation into the function of the BCAR3 protein.

Acknowledgments This work was supported in part by JSPS KAKENHI, Grant Number 24500496.

References

Agrawal N, Nayak DP, Haripriya A, Bhuwania P (2015) Phacoemulsification with toric IOL implantation in Alport syndrome with anterior lenticonus having spontaneously ruptured anterior capsule. Eur J Ophthalmol 25:e78–e80

Bassnett S, Mataic D (1997) Chromatin degradation in differentiating fiber cells of the eye lens. J Cell Biol 137:37–49

Cai D, Iyer A, Felekkis KN, Near RI, Luo Z, Chernoff J, Albanese C, Pestell RG, Lerner A (2003) AND-34/BCAR3, a GDP exchange factor whose overexpression confers antiestrogen resistance, activates Rac, PAK1, and the cyclin D1 promoter. Cancer Res 63:6802–6808

Gotoh T, Cai D, Tian X, Feig LA, Lerner A (2000) p130Cas regulates the activity of AND-34, a novel Ral, Rap1, and R-Ras guanine nucleotide exchange factor. J Biol Chem 275:30118–30123

Graw J (2004) Congenital hereditary cataracts. Int J Dev Biol 48:1031–1044

Graw J (2009) Mouse models of cataract. J Genet 88:469–486

Graw J, Neuhäuser-Klaus A, Löster J, Favor J (2002) A 6-bp deletion in the Crygc gene leading to a nuclear and radial cataract in the mouse. Invest Ophthalmol Vis Sci 43:236–240

Gray W, Sponsel WE, Scribbick FW, Stern AR, Weiss CE, Groth SL, Walker JD (2011) Numerical modeling of paintball impact ocular trauma: identification of progressive injury mechanisms. Invest Ophthalmol Vis Sci 52:7506–7513

Grove M, Demyanenko G, Echarri A, Zipfel PA, Quiroz ME, Rodriguiz RM, Playford M, Martensen SA, Robinson MR, Wetsel WC, Maness PF, Pendergast AM (2004) ABI2-deficient mice exhibit defective cell migration, aberrant dendritic spine morphogenesis, and deficits in learning and memory. Mol Cell Biol 24:10905–10922

Kang M, Cho JW, Kim JK, Kim E, Kim JY, Cho KH, Song CW, Yoon SK (2008) Fine localization of a new cataract locus, Kec, on mouse chromosome 14 and exclusion of candidate genes as the gene that causes cataract in the Kec mouse. BMB Rep 41:651–656

Kohale K, Ingle A, Kelkar A, Parab P (2004) Dense cataract and microphthalmia–new spontaneous mutation in BALB/c mice. Comp Med 54:275–279

Kondo T, Nagai H, Morioka H, Kusakabe KT, Okada T (2010) Novel cataract mouse model using ddY strain: hereditary and histological characteristics. J Vet Med Sci 72:203–209

Kondo T, Ishiga-Hashimoto N, Nagai H, Takeshita A, Mino M, Morioka H, Kusakabe KT, Okada T (2011) An increase in apoptosis and reduction in αB-crystallin expression levels in the lens underlie the cataractogenesis of Morioka cataract (MCT) mice. Med Mol Morphol 44:221–227

Kondo T, Ishiga-Hashimoto N, Nagai H, Takeshita A, Mino M, Morioka H, Kusakabe KT, Okada T (2014a) Expression of transforming growth factor β and fibroblast growth factor 2 in the lens epithelium of Morioka cataract mice. Congenit Anom (Kyoto) 54:104–109

Kondo T, Nagai H, Kawashima T, Taniguchi Y, Koyabu N, Takeshita A, Kusakabe KT, Okada T (2014b) Hereditary and histologic characteristics of the CF1/b cac mouse cataract model. Comp Med 64:360–368

Liu Y, Zhang X, Luo L, Wu M, Zeng R, Cheng G, Hu B, Liu B, Liang JJ, Shang F (2006) A novel alphaB-crystallin mutation associated with autosomal dominant congenital lamellar cataract. Invest Ophthalmol Vis Sci 47:1069–1075

Mace PD, Wallez Y, Dobaczewska MK, Lee JJ, Robinson H, Pasquale EB, Riedl SJ (2011) NSP-Cas protein structures reveal a promiscuous interaction module in cell signaling. Nat Struct Mol Biol 18:1381–1387

Maeda YY, Funata N, Takahama S, Sugata Y, Yonekawa H (2001) Two interactive genes responsible for a new inherited cataract (RCT) in the mouse. Mamm Genome 12:278–283

Makkinje A, Vanden Borre P, Near RI, Patel PS, Lerner A (2012) Breast cancer anti-estrogen resistance 3 (BCAR3) protein augments binding of the c-Src SH3 domain to Crk-associated substrate (p130cas). J Biol Chem 287:27703–27714

McAvoy JW, Chamberlain CG, de Iongh RU, Hales AM, Lovicu FJ (1999) Lens development. Eye (Lond) 13(Pt 3b):425–437

Narita M, Wang Y, Kita A, Omi N, Yamada Y, Hiai H (2002) Genetic analysis of Nakano Cataract and its modifier genes in mice. Exp Eye Res 75:745–751

Near RI, Smith RS, Toselli PA, Freddo TF, Bloom AB, Vanden Borre P, Seldin DC, Lerner A (2009) Loss of AND-34/BCAR3 expression in mice results in rupture of the adult lens. Mol Vis 15:685–699

Okamura T, Miyoshi I, Takahashi K, Mototani Y, Ishigaki S, Kon Y, Kasai N (2003) Bilateral congenital cataracts result from a gain-of-function mutation in the gene for aquaporin-0 in mice. Genomics 81:361–368

Quinlan RA (2015) Drug discovery. A new dawn for cataracts. Science 350:636–637

Schrecengost RS, Riggins RB, Thomas KS, Guerrero MS, Bouton AH (2007) Breast cancer antiestrogen resistance-3 expression regulates breast cancer cell migration through promotion of p130Cas membrane localization and membrane ruffling. Cancer Res 67:6174–6182

Singh DP, Guru SC, Kikuchi T, Abe T, Shinohara T (1995) Autoantibodies against beta-crystallins induce lens epithelial cell damage and cataract formation in mice. J Immunol 155:993–999

Smith RS, Sundberg JP, Linder CC (1997) Mouse mutations as models for studying cataracts. Pathobiology 65:146–154

Song CW, Okumoto M, Mori N, Yamate J, Sakuma S, Kim JS, Han SS, Hilgers J, Esaki K (1997) A new hereditary cataract mouse with lens rupture. Lab Anim 31:248–253

Sun G, Cheng SY, Chen M, Lim CJ, Pallen CJ (2012) Protein tyrosine phosphatase α phosphotyrosyl-789 binds BCAR3 to position Cas for activation at integrin-mediated focal adhesions. Mol Cell Biol 32:3776–3789

Teramoto Y, Uga S, Matsushima Y, Shimizu K, Morita T, Shirakawa S (2000) Morphological study on rupture of posterior capsule in RLC mouse lens. Graefes Arch Clin Exp Ophthalmol 238:970–978

Vanden Borre P, Near RI, Makkinje A, Mostoslavsky G, Lerner A (2011) BCAR3/AND-34 can signal independent of complex formation with CAS family members or the presence of p130Cas. Cell Signal 23:1030–1040

Wallez Y, Riedl SJ, Pasquale EB (2014) Association of the breast cancer antiestrogen resistance protein 1 (BCAR1) and BCAR3 scaffolding proteins in cell signaling and antiestrogen resistance. J Biol Chem 289:10431–10444